EDITORIAL CSIC

Materiales de Construcción
76 (361) January-March 2026, e406
ISSN-L: 0465-2746, eISSN: 1988-3226
https://doi.org/10.3989/mc.2026.393224

ARTICLE

Alkaline activated concrete with recycled asphalt pavement aggregate

Hormigón activado alcalinamente con árido de pavimento asfáltico reciclado

S. Sharma
Department of Civil Engineering, Dr. B. R. Ambedkar National Institute of Technology (Jalandhar, India)
sajans.ce.22@nitj.ac.in, https://orcid.org/0009-0000-0662-0583

S. Bawa
Department of Civil Engineering, Dr. B. R. Ambedkar National Institute of Technology (Jalandhar, India)
Corresponding author: bawas@nitj.ac.in, https://orcid.org/0000-0002-8831-0841

Abstract: Geopolymer concrete is an eco-friendly alternative to cement concrete that reduces carbon emissions through the utilisation of industrial waste. This study enhances its sustainability by incorporating recycled asphalt pavement (RAP) aggregates as partial replacements for natural coarse aggregate at 0%, 20%, 40%, 60%, 80%, and 100%, using fly ash and dolomite as binders. The analysis revealed improvements within a specific RAP threshold, with 40% identified as the optimum proportion. Strong correlations ($R^2 > 0.90$) were observed among compressive, flexural, split tensile strength and ultrasonic pulse velocity at 28 and 56 days. SEM-EDS analyses indicated a denser matrix, while XRD and FTIR confirmed the formation of C(N)–A–S–H type gels. These findings demonstrate the potential of RAP in geopolymer concrete, promoting sustainable construction through efficient material reuse.

Keywords: Geopolymer concrete; Recycled asphalt pavement aggregates; Dolomite; Fly Ash; Microstructure analysis.

Resumen: El hormigón geopolimérico es una alternativa ecológica al hormigón con cemento que reduce las emisiones de carbono mediante el aprovechamiento de residuos industriales. Este estudio mejora su sostenibilidad incorporando áridos reciclados de pavimento asfáltico (RAP) como sustitutos parciales del árido grueso natural en proporciones de 0%, 20%, 40%, 60%, 80% y 100%, utilizando ceniza volante y dolomita como aglutinantes. El análisis reveló mejoras dentro de un umbral específico de RAP, identificándose el 40% como la proporción óptima. Se observaron fuertes correlaciones ($R^2 > 0.90$) entre la resistencia a compresión, flexión, tracción indirecta y la velocidad del pulso ultrasónico a los 28 y 56 días. Los análisis SEM-EDS indicaron una matriz más densa, mientras que XRD y FTIR confirmaron la formación de geles del tipo C(N)–A–S–H. Estos resultados demuestran el potencial del RAP en el hormigón geopolimérico, promoviendo la construcción sostenible mediante la reutilización eficiente de materiales.

Palabras clave: Hormigón geopolimérico; Áridos de pavimento asfáltico reciclado; Dolomita; Cenizas volantes; Análisis microestructural.

Received: 20-08-2024 / **Accepted**: 26-12-2025 / **Published**: 29-06-2026

Citation: Sharma S, Bawa S. 2026. Alkaline activated concrete with recycled asphalt pavement aggregate. *Mater. Construcc.* 76(361):e406. https://doi.org/10.3989/mc.2026.393224

Supplementary information ↓

GRAPHICAL ABSTRACT

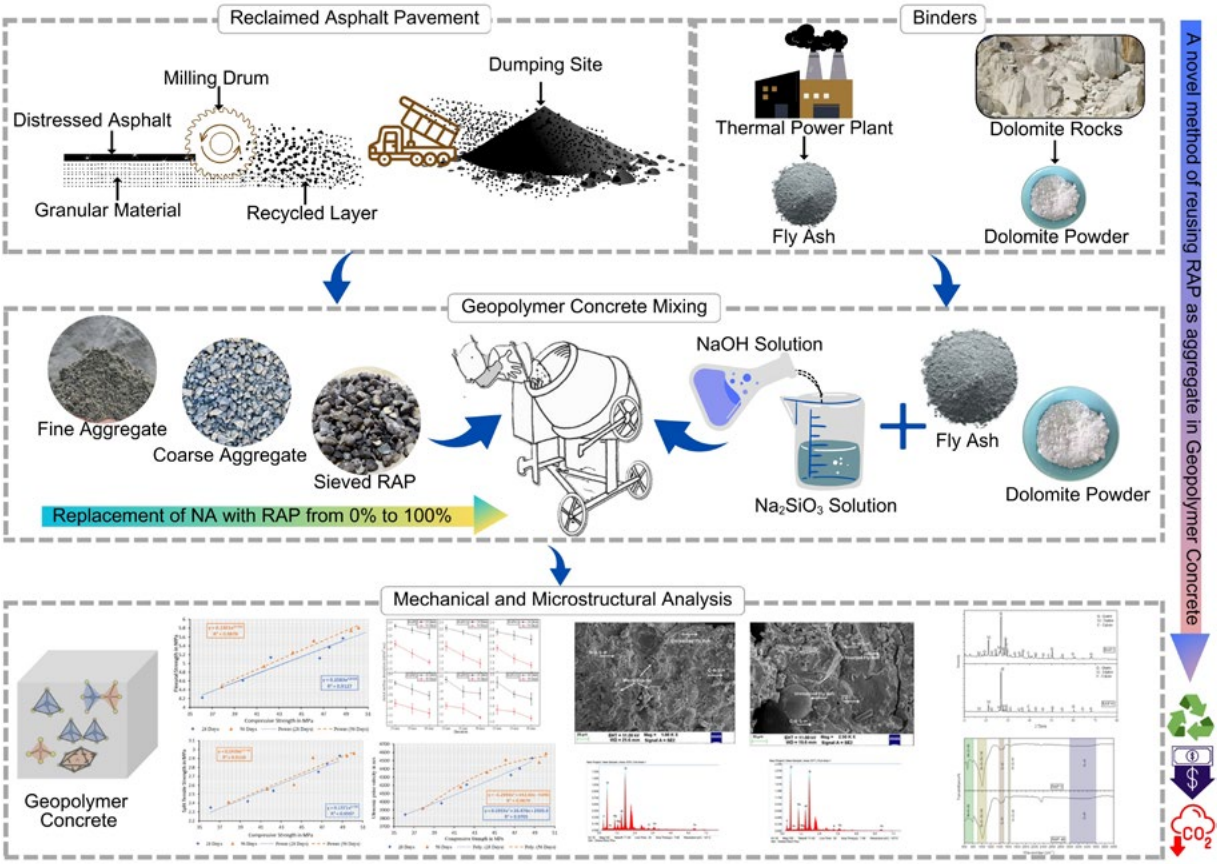

1. INTRODUCTION AND BACKGROUND

The swift construction and ease of maintenance make flexible or asphalt pavements a popular choice for road construction. In contrast to rigid pavement, they offer a cost-effective solution with a smooth, quiet, and safer riding experience along with durable performance. According to a report by the National Asphalt Pavement Association (NAPA), asphalt is employed in 94% of U.S. pavements, whether in full-depth construction or as an overlay (1). Additionally, (2) a report said that 78% of urban roadways and 86% of rural highways in the United States have flexible pavement.

The majority of runways across the globe, including the Autobahn in Germany, have flexible pavements. In the process of removing or scraping worn-out and aged flexible pavement, recycled asphalt pavement (RAP) waste material is produced. RAP is typically broken down into chunks, then processed and used in new asphalt mixes for road construction and repairs. In the United States, RAP recycling was estimated to be up to 89.2 million tons in 2019 (3). However, the European Asphalt Pavement Association (EAPA 2020) report states that the European Union recycled 50 million tonnes of RAP, and in 2016, China used more than 60 million tonnes of RAP (3). A hot mix asphalt mixture containing 15% to 40% RAP will result in a cost reduction of between $6.80 and $3.40 per tonne (4).

There were reported $300 million in cost reductions due to the addition of 30 million tonnes of RAP to hot mix asphalt (5). Utilising RAP has a positive impact on the environment since it minimises roadside waste and eases the difficulties of authorities involved in disposing of RAP waste (3). Combining RAP with other virgin or recycled materials has been tried by researchers as a way to incorporate it into pavement base and subbase materials; however, these mixtures typically fall short of the required minimum strength and durability standards (6, 7).

RAP application in concrete promotes natural resource preservation and reduces roadside or landfill disposal. Researchers have conducted a number of studies to analyse the effect of using RAP aggregate in concrete. It is observed that abrasion and attrition treated RAP inclusive concrete mixes strengthen mechanical and durability properties by substituting OPC with 10% silica fumes (SF10) and fly ash (FA) up to 20% and 5% with sugarcane bagasse ash (SCBA) (8). SF10 exhibited only a slight 5% compressive strength reduction; microanalysis confirmed a denser Interfacial Transition Zone (ITZ) and improved performance in SF and FA mixes (8). Recycled concrete aggregate (RCA) and RAP were combined with natural aggregate (NA) to examine the mechanical characteristics of concrete at different temperatures (20°C, 200°C, 400°C, and 500°C). The recommended recycled mixture for usage at high temperatures is 90% NA and 10% RAP, 90% RCA, and 10% RAP for different mixtures (9). According to the findings, compressive, elasticity modulus, splitting tensile, and flexural properties decrease when temperature or the replacement levels of RAP and RCA increase (9). In another study, RAP and precast concrete waste aggregate fully replaced natural aggregates (NA) in structural concrete, alongside the addition of 35% ground granulated blast furnace slag (GGBS) (10).

According to findings by the researchers, recycled aggregates from old precast concrete can still maintain a sufficient level of strength for structural applications. However, RAP aggregates have higher flexural strength than compressive strength, making them appropriate for non-structural applications (10).

RAP aggregate is used to replace up to 40% of the coarse particles in self-consolidating concrete (SCC) in order to make it more environmentally friendly. A decline in compressive and tensile strength is observed with an increase in the dosage of RAP (11). A slag dosage of 30% shows higher strength than the fly ash range of 20-30% (11). Concrete containing supplementary cementitious material (SCM) exhibits less shrinkage, but unrestrained shrinkage increases with RAP content.

Furthermore, beams without RAP had the maximum load-bearing capability, whereas both the fly ash (20-30%) and slag (30%) increased stiffness, suggesting possible uses for sustainable SCC (11). A deep beams study containing NA, RCA, and RAP shows that replacing NA with 50% of RCA, RCA, and RAP reduces shear capacity by 9-11.7% and 4.66-7.52%, respectively (12). The shear capacity observed equals the change in mix design when 100% NA is replaced with RCA and RAP. RAP beams exhibit higher absorbed energy. Compared to NCA specimens, RAP deep beams exhibited more flexural but fewer diagonal fractures with smaller widths and spacing (12). According to this research, increasing RAP concentration from 0% to 100% has a detrimental influence on workability and compressive strength. Optimal strain and fracture rates rise while the curve of optimum strain and elastic modulus declines (13). These studies show that RAP works well when incorporated with NA and other RCA in lower percentages. Still, when used in higher percentages, it reduces durability as well as compressive and tensile strength. Given the ongoing production of RAP from road sector expansion and its repair, using a large amount of RAP is crucial to prevent it from stacking up as useless material on the roadside or in dumps.

According to the prediction, carbon dioxide emissions will significantly increase with an increase in global cement output to 6.1 billion metric tonnes in 2051, at a rate of 1 tonne of CO_2 emissions for every metric tonne of cement produced. This projection highlights the necessity for the cement sector to employ sustainable practices and emissions reduction strategies (14). An environmentally friendly substitute for conventional cement-based concrete is geopolymer concrete. Inorganic mineral compounds are used in the production of geopolymer concrete, which removes the need for further natural resource consumption and the release of CO_2 into the environment. These inorganic mineral compounds are produced as by-products in the metallurgical, power, and electro-metallurgical sectors (15). When compared to traditional cement-based concrete, the usage of Geopolymer Concrete (GPC) is anticipated to result in significant energy savings of up to 43% and a spectacular reduction in greenhouse gas emissions of up to 80% (16). An alkaline solution is combined with an alkali-activated binder, which is generally high in silica and alumina content, such as substances like fly ash, slag, etc.

(16). Numerous benefits of geopolymer concrete include its remarkable strength, fire resistance, durability, and low carbon footprint. However, using NA in the production of geopolymer concrete increases both prices and the use of natural resources.

The incorporation of RAP aggregate in GPC production not only aids in waste reduction, which is a significant environmental concern, but also contributes to mitigating its adverse effects. The feasibility of incorporating RAP in pavement base course blends can be stabilised with fly ash, achieving a compressive strength greater than 4.5 MPa and fulfilling the requirements for design strength in cemented base materials.

Durability tests, including wet/dry cycles, showed a weight loss of less than 14%, with leachate analysis indicating minimal environmental impact, with an almost tenfold reduction in pH, calcium, and sodium ion concentration after four cycles (17). The durability of RAP and FA chemicals under wetting-drying (w-d) cycles is being studied in this research. Unconfined Compression Strength (UCS) tests show that the UCS test of the RAP-FA mix improves with up to six w-d cycles, with triggered reactions producing more C-A-S-H in results. The coexistence of the geopolymerisation products N-A-S-H and C-A-S-H causes the RAP-FA geopolymer to exhibit an increase in initial strength in the first six w-d cycles. After six cycles, more crack propagation results in a decline in strength. A stable alumino-silicate polymer structure, which is enhanced by a higher NaOH concentration, increases durability (18, 19).

Researchers investigated the strength and durability of RAP-FA mixtures employing roller-compacted geopolymer concrete (RCGPC). It has been analysed that increasing the curing period to 48 hours under 60°C results in achieving 100% compressive strength and elastic modulus in 28 days. The split tensile strength increases by 10% when the molarity is raised from 8 to 10. Compared to RAP-RCC with conventional cement, RAP-RCGPC displays considerably higher split tensile strength and UCS, up to 60% and 28%, respectively (20). In another research, the performance of GPC with a high dosage of RAP content for pavement construction is analysed compared to conventional cement concrete. The findings show that RAP-geopolymer concrete has superior compressive, flexural, and split tensile strengths to RAP-cement concrete and has high durability. Significant variables include the incorporation of 10% more fines, an 8M NaOH solution, and Na_2SiO_3/NaOH of 1:1. Critical curing for 48 hours at a temperature of 60°C exhibits superior tensile strength and better bonding with RAP aggregates (21).

This research addresses a gap in the existing literature by investigating different replacement ratios of RAP in geopolymer concrete with fly ash and dolomite as binder materials. RAP integration into geopolymer concrete requires meticulous procedures to optimise its performance. The characteristics of RAP are significantly influenced by the source of waste material, which in turn impacts its properties within the geopolymer matrix. Various recycling methods introduce complexities related to sorting efficiency and the overall sustainability of the process. Pretreatment protocols are essential to mitigate impurities and attain high-performance standards. Coarse RAP particles play a crucial role in the Geopolymer concrete mixture's volumetric properties and load-bearing capacity. The intricate nature of the interfacial transition zone between RAP and the geopolymer binder requires careful consideration. Quality control measures, including specific gravity, fineness modulus and water absorption assessments, are imperative to regulate impurities and extraneous materials, aiming for levels below 1%. Additionally, meticulous attention to suitable gradation and particle size distribution is essential to enhance the geopolymer concrete blend's compactness and overall performance characteristics with RAP. It resolves the issue with the tensile and fracture characteristics of geopolymer concrete with RAP.

This study comprehensively examines different properties of RAP-geopolymer concrete through specimen testing for compression, flexural, splitting tensile, initial surface absorption, and ultrasonic pulse velocity, incorporating varying dosages of RAP in geopolymer concrete. To gain a thorough knowledge of the material's characteristics, morphological studies employing scanning electron microscopy (SEM), energy dispersive X-ray spectroscopy (EDS), X-ray diffraction (XRD), and Fourier transform infrared spectroscopy (FTIR) methods are also carried out. This research presents valuable, novel insights into the feasibility of RAP-geopolymer concrete as a construction material.

2. MATERIALS AND METHODS

2.1. Materials and material properties

The RAP incorporated in geopolymer concrete for this research is recovered from local roadside dumps near Amritsar (Jandiala Guru), Punjab, India. RAP collected from the site is in the form of blocks or sections of asphalt pavement. These asphalt blocks are crushed and graded using 4.75 mm to 12.5 mm sieves. Specific gravity (G), fineness modulus (FM), and water absorption (WA) of different materials are tested as per ASTM C127 (22), ASTM C128 (23), and ASTM C136 (24). Tested specific gravity, fineness modulus, and water absorption for RAP aggregate are 2.34, 3.14, and 0.95%. Fine and coarse aggregates are supplied from a local distributor and washed and sun-dried before use. The grading of coarse aggregate used has been maintained the same as that of RAP aggregate. Tested G, FM and WA for fine aggregate are 2.47, 2.54, and 1.62%, whereas for coarse aggregate, G = 2.55, FM = 5.86, and WA = 2.12%. Fly ash (FA) used for this research work is supplied from the thermal power plant in Ropar, Punjab. Natural dolomite (DO) is purchased from a local supplier for this work. Tested G and FM for fly ash are 2.66 and 2.12, respectively. In contrast, tested values for dolomite are G = 2.84 and FM = 1.34 in accordance with ASTM C128 (23) and ASTM C430 (25).

The significant components of fly ash tested are 50.51% SiO_2, 24.81% Al_2O_3, 7.16% Fe_2O_3, and 6.52% CaO. In accordance with ASTM C618-12a (26), the fly ash was referred to as a Class F standard due to a total chemical composition of SiO_2 + Al_2O_3 + Fe_2O_3 exceeding 70 percent. The chemical composition of dolomite comprises 20.58% SiO_2, 8.45% Al_2O_3, 2.75% Fe_2O_3, and 34.58% CaO. Similarly, the recycled asphalt pavement showed the main chemical composition of 37.11% SiO_2, 13.72% Al_2O_3, 5.18% Fe_2O_3, and 24.74% CaO. The elevated amount of CaO content in both RAP and natural dolomite is expected to influence the alkalinity of the system, which can facilitate the activation of silicate and aluminate species. In the case of RAP and dolomite, the presence of CaO may contribute to the formation of a high-pH environment conducive to the dissolution of silica and alumina from the fly ash. However, it should be noted that the reactivity of calcium compounds in these materials is contingent upon their phase. While CaO and $Ca(OH)_2$ are known to exhibit substantial reactivity under alkaline conditions, the calcium carbonates ($CaCO_3$) and magnesium carbonates ($MgCO_3$) found in dolomite are essentially inert in their natural state and exhibit limited reactivity unless subjected to fine grinding or elevated temperatures. Therefore, the role of CaO in RAP and dolomite is more pertinent to the alkaline activation process. In accordance with ASTM C618-12a (26) and ASTM C25 (27), the chemical composition of FA, DO, and RAP is shown in Table 1.

Table 1. Chemical compositions of the recycled waste material.

Material Type	Chemical Composition of Material (%)						
	SiO_2	Al_2O_3	Fe_2O_3	CaO	MgO	SO_3	K_2O
Fly Ash	50.51	24.81	7.16	6.52	2.32	1.72	2.51
Dolomite	20.58	8.45	2.75	34.58	20.48	1.45	1.12
RAP	37.11	13.72	5.18	24.75	0.42	0.23	1.35

2.2. Sample preparation

The sodium hydroxide (NaOH) used for this research is bought in flakes having a density of 2.14 with pH of 13-14, Na content of 58%, O content of 40%, H content of 2% and is white in colour. The required amount of sodium hydroxide flakes for a 1-litre water solution must be calculated for a specified molar concentration of NaOH solution. To produce a 1M NaOH solution, 40 grams of NaOH flakes are mixed into distilled water until the solution reaches a final volume of 1 litre. In the laboratory, a 10M NaOH solution is prepared by dissolving NaOH flakes (98+% pure) in distilled water using the same procedure 24 hours prior to casting.

For this research, a commercially available technical-grade sodium silicate (Na_2SiO_3) solution is used. The density of Na_2SiO_3 is 1.55 with pH 13-14, Na content 9%, O content 27%, H content 64% and is off-white in colour, with a composition of 36% solids (comprising 27% SiO_2 and 9% Na_2O) and 64% water by weight. The Na_2SiO_3 solution, with a SiO_2/Na_2O ratio 2.95, is mixed with the NaOH solution. The Na_2SiO_3/NaOH ratio of 1.55 is used to create the alkaline solution required for the geopolymer concrete.

Table 2. Mix design of geopolymer concrete (kg/m³).

Mix	FA	DO	Fine	NA	RAP	NaOH Sol.	Na_2SiO_3 Sol.
RAP0	350	150	600	1250	0	88.24	136.76
RAP20	350	150	600	1000	250	88.24	136.76
RAP40	350	150	600	750	500	88.24	136.76
RAP60	350	150	600	500	750	88.24	136.76
RAP80	350	150	600	250	1000	88.24	136.76
RAP100	350	150	600	0	1250	88.24	136.76

For the preparation of the geopolymer concrete testing sample, an alkaline solution mixture of Na_2SiO_3 and NaOH is blended 30 minutes prior to being mixed with binders (FA and DO). Initially, fine and coarse aggregates on a saturated surface are in a dry state, with binders combined for 5 minutes in the pan mixture. This dry combination of aggregate and binder is then progressively given a dose of alkaline solution. To create a homogeneous consistency, the mixture is mixed for an additional 8–10 minutes. The control mixture, at this moment, referred to as RAP0 (with 0% RAP replacement), serves as a critical baseline for this study and is composed entirely of conventional aggregate with no addition of RAP aggregate. This fundamental blend of RAP0 serves as a standard for structured assessments of the various mix compositions, which include progressive RAP aggregate inclusion levels of 20%, 40%, 60%, 80%, and 100%. The usage of 10M NaOH and a Na_2SiO_3/NaOH ratio of 1.55, as well as a constant alkaline/binder ratio of 0.45, are essential parameters that are kept the same throughout all mixes, as shown in Table 2. The concrete samples are then compacted into three layers, with two minutes of rodding and vibration to each layer, as shown in Figure 1.

The specimens are sealed with plastic wrap to avoid moisture loss during curing. The sealed specimens undergo initial ambient curing at room temperature for 24 hrs, followed by subsequent oven curing at 60 °C for 48 hours in the subsequent phase.

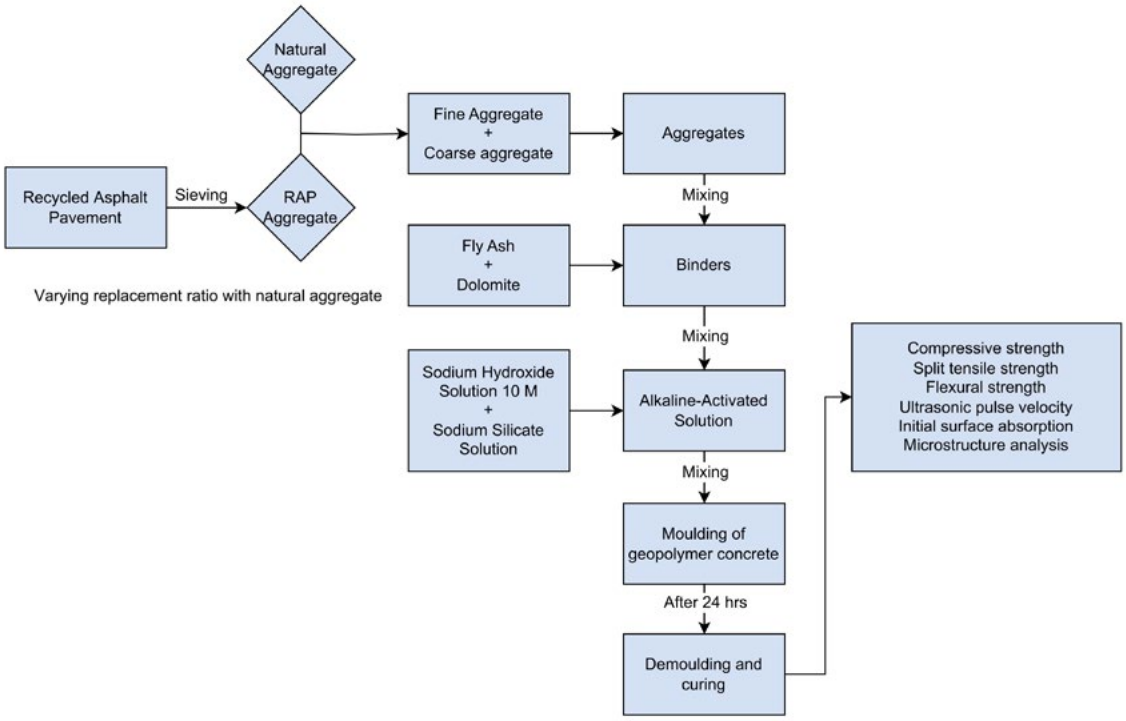

Figure 1. Flow chart for sample preparation and testing.

2.3. Experimental design parameters

As mentioned earlier, a number of experiments were performed on the GPC mixes with various amounts of RAP aggregate inclusion in place of conventional aggregate. Activated fly ash and dolomite are added to these mixtures to analyse their strength. The subsequent sections provide details on the different tests performed and the corresponding methodologies employed in this research work.

2.3.1. Mechanical properties

In the context of civil engineering, mechanical properties serve as fundamental characteristics that define the reaction of material mass to externally applied loads. For a thorough assessment of material performance, such as geopolymer concrete, essential mechanical tests are conducted to ascertain concrete viability. In accordance with IS 516 (28), the specimen of 150 mm x 150 mm x 150 mm is cast for the compressive strength test. To minimise experimental variation, the average tested value of a minimum of three specimens per mix combination is considered for robust research. The maximum allowable deviation must not exceed ± 2% of the maximum load. Equation [1] is used for calculating the compressive strength of GPC:

$$S_c = \frac{P_{max}}{A} \qquad [1]$$

Where:

Sc = Compressive strength, P_{max} = Maximum load at failure, A = Cross-sectional area.

Prismatic beam specimens of size 100 mm x 100 mm x 500 mm in accordance with IS 516 (28) are used to evaluate the flexural strength of GPC. Four-point loading is applied at an axial rate of 180 kg/min using a Material Testing System (MTS). The rollers at the machine's base are arranged with a centre-to-centre distance of 400 mm. The load application is executed through two similar rollers situated at the third point of the supporting span, with a centre-to-centre spacing of 133 mm. The acceptable margin of error in the applied load should not exceed ±0.5%. Equations [2] and [3] are used for calculating the flexural strength of GPC:

$$Fs = \frac{PL}{bd^2} \qquad [2]$$

$$Fs = \frac{3Pa}{bd^2} \qquad [3]$$

Where:

Fs = Modulus of rupture, P = Applied load, L = Span length, b = Width of the specimen, d = Depth of the specimen, a = Average distance between the line of fracture and the nearest support measured on the tension surface of the beam.

For the split tensile test, a cylindrical specimen of Ø150 mm x 300 mm is used in accordance with IS 5816 (29). The load application is gradual and devoid of any sudden shocks, increasing steadily at a nominal rate of 1.51 mm²/minute using a Material Testing System (MTS). Equation [4] is used for calculating the split tensile strength of GPC:

$$St = \frac{2P}{\pi L Ø} \qquad [4]$$

Where:

St = Modulus of rupture, P = Applied load, L = Span length, Ø = Diameter of the specimen

2.3.2. Initial surface absorption test

Moisture ingress by absorption or penetration is the main cause of early degradation in concrete, making it a critical measure for the durability of the material. In accordance with BS 1881: Part 208 (30), the Initial Surface Absorption Test (ISAT) analyses uniaxial water penetration in concrete surfaces using three 150 mm x 150 mm x 150 mm GPC cubes per mix. Specimens are dried at 105 ± 5 degrees Celsius until successive 24-hour mass readings differ by 0.1%. Water is introduced by a controlled capillary tube connected to a reservoir. After ten minutes, the flow ceases, allowing the water to retreat. Meniscus movement on the scale is recorded for 1 minute, determining the rate of initial surface absorption (ml/ m^2 s) at 10, 30, and 60-minute intervals.

2.3.3. Ultrasonic pulse velocity

In accordance with ASTM C597-09 (31), the Ultrasonic Pulse Velocity (UPV) test is conducted using electro-acoustical transducers emitting a 55 KHz frequency from one end of the concrete specimen and receiving it on the opposing end. For each GPC mix, three specimens of size 100 mm x 100 mm x 100 mm are used for analysis. To optimise signal transmission, a thin layer of coupling gel is applied to the test faces of specimens. The resulting velocity, determined using Equation [5], serves as a critical parameter, where higher velocities correlate with superior quality of concrete, while lower velocities correlate with inferior quality.

$$\mathrm{Pv} = \frac{\mathrm{L}}{\mathrm{t}} \qquad [5]$$

Where:

Pv = Pulse velocity, m/s, L = Distance between centres of transducer faces (m), t = Transit time (s).

2.3.4. Microstructural and mineralogical analyses

Advanced characterisation techniques are used to analyse the microstructure and mineralogy of geopolymer concrete with NA and incorporated with RAP aggregate. Solid specimens were extracted from the core region of geopolymer concrete samples after 56 days of curing and mechanical testing to ensure representative internal microstructural features. Microstructural analysis was conducted using a SIGMA 500VP Field Emission Scanning Electron Microscope (FE-SEM), operated at an accelerating voltage of 6–12 kV.

The use of a low-vacuum mode enabled high-resolution imaging across the full width of the specimens by avoiding additional damage to the fragile concrete matrix. This approach facilitated detailed examination of the geopolymer matrix, reaction products, and interfacial transition zones (ITZ) between the binder and aggregates, thereby providing valuable insights into the morphological development and phase distribution within the 56-day geopolymer concrete. The same specimens were further analysed using integrated Energy-Dispersive X-ray Spectroscopy (EDS) to accurately determine the elemental composition and spatial distribution of key constituents within the microstructure. Phase analysis of the geopolymer concrete (GPC) specimens was carried out using a PANalytical Empyrean X-ray Diffraction (XRD) system, equipped with a high-performance 4 kW X-ray generator operating at a maximum of 60 kV and 100 mA. The instrument features a precision-engineered goniometer with a wide scanning range of $-111° < 2\theta < 168°$, with the smallest addressable increment of 0.0001°, and angular reproducibility less than 0.0002°. Finely ground powder samples were extracted from the core region of 56-day cured and tested GPC specimens to ensure representative characterisation. The primary objective was to identify and quantify the crystalline phases present, providing insights into the reaction products and phase assemblages within the geopolymeric matrix.

Fourier Transform Infrared (FTIR) spectroscopy was performed using a Bruker Alpha spectrometer to investigate the chemical bonding and functional groups present in the geopolymer matrix. Spectral data were recorded within the infrared region, ranging from 4000 to 500 cm^{-1}, targeting characteristic vibrational bands associated with aluminosilicate structures. Specimens of a 56-day cured geopolymer concrete sample were finely ground to a particle size less than 75 µm to ensure homogeneity and adequate infrared absorption. Approximately 2-3 g of the sample was inserted into the infrared equipment, with software activation using specified parameters. This comprehensive analysis provides deep insights into the material's microstructure, composition, and chemical properties, thus offering comparative information on the suitability and performance of GPC with NA and RAP aggregate in a variety of applications.

3. RESULTS AND DISCUSSIONS

3.1. Correlation between compressive strength and flexural strength

Compressive strength and flexural strength are two critical mechanical properties of concrete. Increased compressive strength frequently results in higher flexural strength; hence, there is usually a positive correlation between the two most important mechanical properties. The reason is that the quality and strength of the concrete matrix influence both mechanical attributes. The compressive strength and flexural strength test results for different GPC mix designs at both 28 and 56 days, along with their standard deviations, are shown in Figure 2. RAP40 mix (with 40% RAP replacement) in comparison with RAP0 (with 0% RAP replacement) showed the highest compressive strength, with a maximum of 48.75 MPa at 28 days and 50.14 MPa at 56 days. RAP0, RAP20, and RAP60 also show competitive strengths ranging from 46.65 MPa to 47.52 MPa at 28 days and 46.13 MPa to 49.45 MPa at 56 days. In contrast, RAP80 and RAP100 display reduced compressive strengths of 39.74 MPa and 36.12 MPa at 28 days of age and 41.65 MPa and 37.86 MPa at 56 days of age, respectively. Similar trend was also observed in flexural strength, RAP40 displaying highest strength 5.57 MPa at 28 days and 5.81 MPa at 56 days, compare to RAP0 with no RAP aggregate. RAP0 and RAP20 follow closely, with strengths of 5.12 MPa and 5.37 MPa at 28 days and 5.75 MPa and 5.52 MPa at 56 days, respectively. However, RAP60, RAP80, and RAP100 experience a drop in flexural strength, ranging from 4.22 MPa to 5.14 MPa at 28 days and 4.47 MPa to 5.25 MPa at 56 days, as shown in Figure 2.

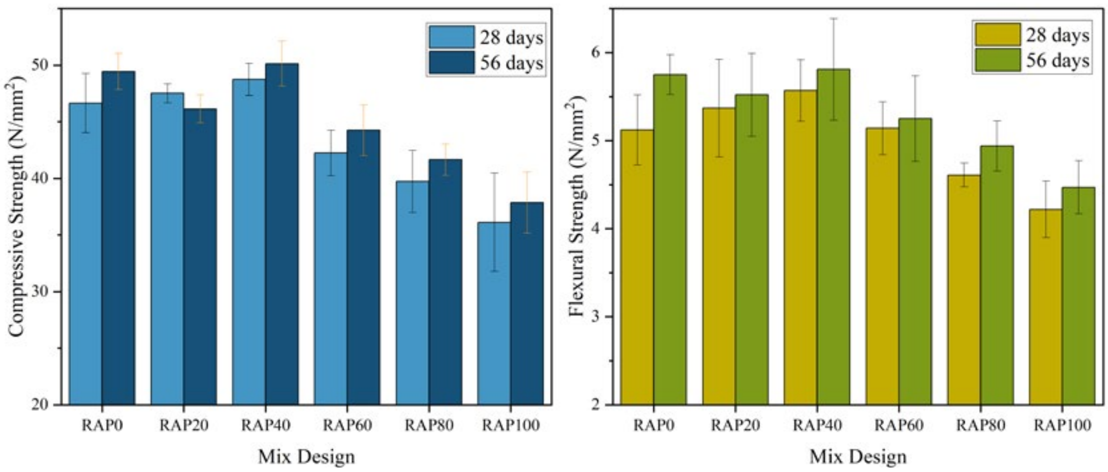

Figure 2. Compressive strength and Flexural strength of specimens at 28 days and 56 days (N/mm^2).

The observed increase in compressive strength for the RAP40 mix may be attributed to the dual effect of aggregate morphology and RAP aggregates' surface characteristics. While the angular and crushed nature of RAP particles promotes mechanical interlock and contributes to improved packing density, the residual bitumen coating on the aggregate surface may also influence the microstructural development in higher replacement levels (32). This bituminous layer can act as a diffusion barrier, potentially moderating alkali-silica reactions and altering geopolymer gel formation near the interface. However, in the current study, the dense matrix is also observed via SEM and the broadened FTIR bands in RAP40 indicate successful geopolymerisation despite this coating aligning with mechanical performance, as shown in Figure 9 and 11. Partial RAP replacement up to a specific limit resulted in improved interfacial bonding and strength due to better packing and enhanced matrix continuity.

Thus, the strength gain in RAP40 is likely a synergistic result of mechanical interlocking and chemically favourable conditions promoted by controlled RAP aggregate (33). Using the power equation, the correlation between compressive strength and flexural strength is established, as shown in Figure 3.

For 28 days:

$$Sc = 0.2083(Fs)^{0.8428}, R^2 = 0.9127, [6]$$

For 56 days:

$$Sc = 0.1501(Fs)^{0.9363}, R^2 = 0.9879. [7]$$

Equations [6] and [7] show a significant and credible positive correlation between compressive strength and flexural strength for different RAP aggregate amounts in geopolymer concrete mix designs. The R^2 values display that approximately 91.27% and 98.79% of the variation in compressive strength can be attributed to flexural strength at 28 and 56 days, respectively. These results suggest that when designing a GPC mix with specific compressive strength requirements, focusing on improving flexural strength also results in enhanced compressive strength attributes.

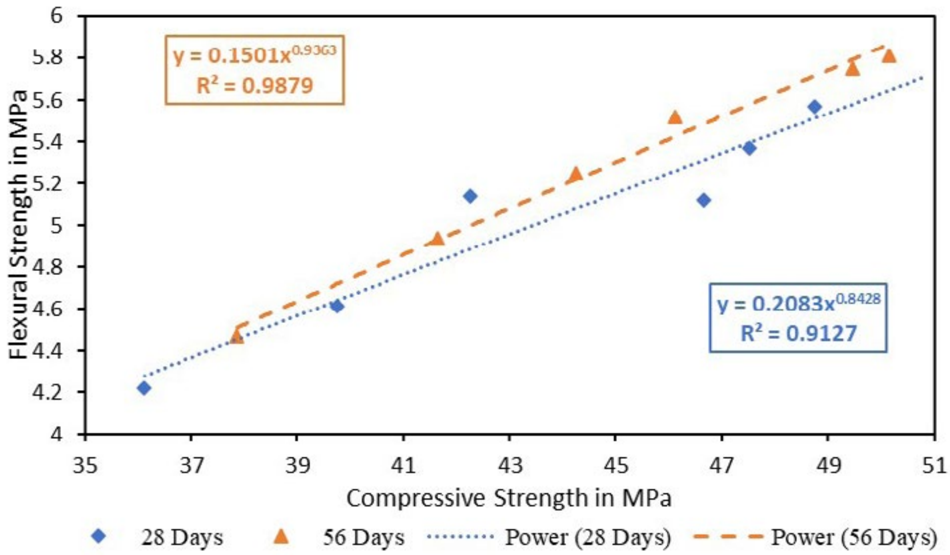

Figure 3. Correlation between Compressive strength (N/mm²) and Flexural strength (N/mm²).

3.2. Correlation between compressive strength and split tensile strength

Compressive strength and split tensile strength are also closely related, as both are indicators of a concrete's overall performance and strength. Increased split tensile strength is frequently a result of higher compressive strength. A comprehensive comparison of compressive strength and split tensile strength test results for GPC mix designs with varying RAP aggregate content at 28 days and 56 days. In terms of compressive strength, RAP40 consistently displays the highest values, reaching 48.75 MPa at 28 days and 50.14 MPa at 56 days. Regarding split tensile strength, RAP40 leads with 2.93 MPa at 28 days and 2.96 MPa at 56 days. RAP0, RAP20, and RAP60 closely follow, with strengths ranging from 2.54 MPa to 2.84 MPa at 28 days and 2.61 MPa to 2.93 MPa at 56 days. However, RAP80 and RAP100 show lower split tensile strengths at 28 days and 56 days, ranging from 2.35 MPa to 2.56 MPa. The split tensile strength result at 28 days and 56 days are shown in Figure 4 along with their standard deviations. The improved mechanical strength of the RAP40 mix can be due to the impact of the aggregate structure and good interfacial transition zone (ITZ) formation. Thereby imparting superior adhesive and bonding within the matrix.

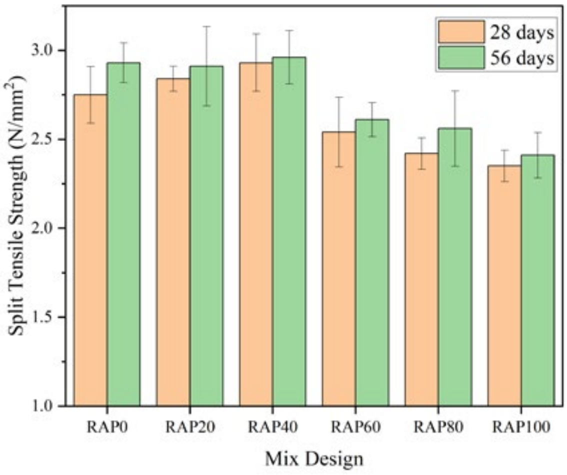

Figure 4. Split tensile strength of specimens at 28 days and 56 days (N/mm²).

Using the power equation, the correlation between the compressive strength and split tensile strength is established, as shown in Figure 5:

For 28 days:

$$Sc = 0.1571\ (St)^{0.748},\ R^2 = 0.9597, \quad [8]$$

For 56 days:

$$Sc = 0.1439\ (St)^{0.7736},\ R^2 = 0.9118. \quad [9]$$

Equations [8] and [9] display a significant and consistent positive correlation between compressive strength and split tensile strength for the geopolymer concrete mix. The R^2 values indicate that approximately 95.97% and 91.18% of the variation in compressive strength can be attributed to split tensile strength at 28 and 56 days, respectively. According to this correlation, increases in split tensile strength are likely to coincide with improvements in compressive strength properties. It is noticeable that the relationship remains strong even at 56 days, proving that this correlation holds as the concrete continues to age.

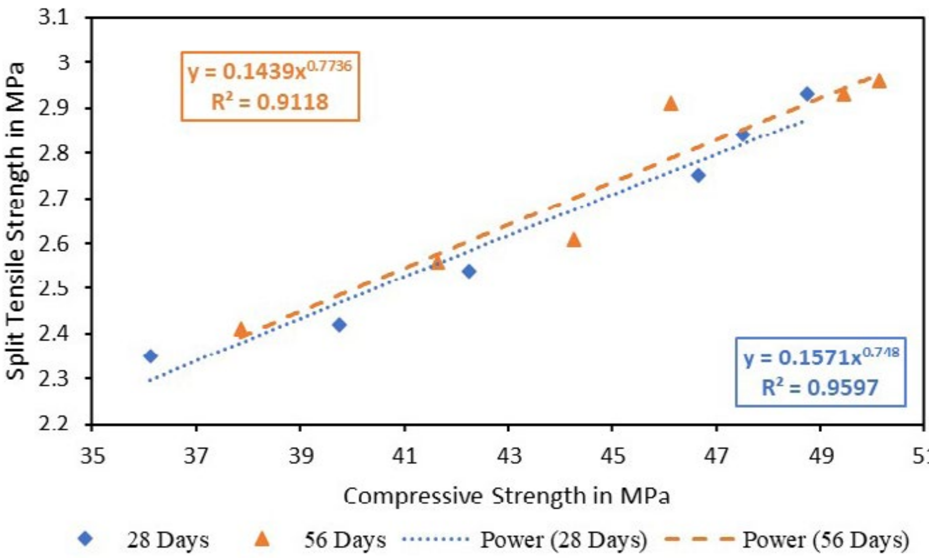

Figure 5. Correlation between Compressive strength (N/mm²) and Split tensile strength (N/mm²).

3.3. Correlation between compressive strength and ultrasonic pulse velocity

The results of the compressive strength and ultrasonic pulse velocity comparison for various GPC mix designs with varying percentages of RAP aggregate at 28 and 56 days. RAP40 consistently demonstrates the highest compressive strengths, with a maximum of 48.75MPa at 28 days and 50.14MPa at 56 days. In the UPV test, a similar trend is observed. RAP40 consistently records the highest UPV values, reaching 4650 m/s at 28 days and 4735 m/s at 56 days. RAP0, RAP20, and RAP60 exhibit relatively high UPV values, ranging from 4110–4405 m/s at 28 days and 4180–4510 m/s at 56 days, indicating good material compactness and internal integrity. This suggests that up to 60% RAP replacement does not significantly compromise the homogeneity or density of the geopolymer matrix. In contrast, RAP80 and RAP100 show noticeably reduced UPV values of 3845–4120 m/s respectively, which may be attributed to the higher content of asphalt binder due to RAP aggregate and possible micro voids at the aggregate-paste interface. The results of UPV at 28 days and 56 days are shown in Figure 6, along with their standard deviations. The bituminous coating on RAP at higher replacement levels can hinder effective geopolymer gel formation and reduce interfacial bonding, leading to a less cohesive matrix and increased porosity. This deterioration in internal structure likely results in lower ultrasonic pulse velocities. Using the power equation, the correlation between compressive strength and ultrasonic pulse velocity is established, as shown in Figure 7.

For 28 days:

$$Sc = 0.2933\,(Pv)^2 + 26.476\,(Pv) + 2503.4,\; R^2 = 0.9705, \quad [10]$$

For 56 days:

$$Sc = -3.2993\,(Pv)^2 + 342.93\,(Pv) - 4346,\; R^2 = 0.9679. \quad [11]$$

These second-order polynomial equations indicate a remarkable correlation between compressive strength and ultrasonic pulse velocity. The high R^2 values of approximately 97.05% and 96.79% at 28 and 56 days, respectively, highlight the strong correlation between these two properties. Equations [10] and [11] show that both linear and non-linear variables influence the correlation. This suggests that ultrasonic pulse velocity can serve as a trustworthy indicator of compressive strength, especially when combined with the given equations for certain concrete ages.

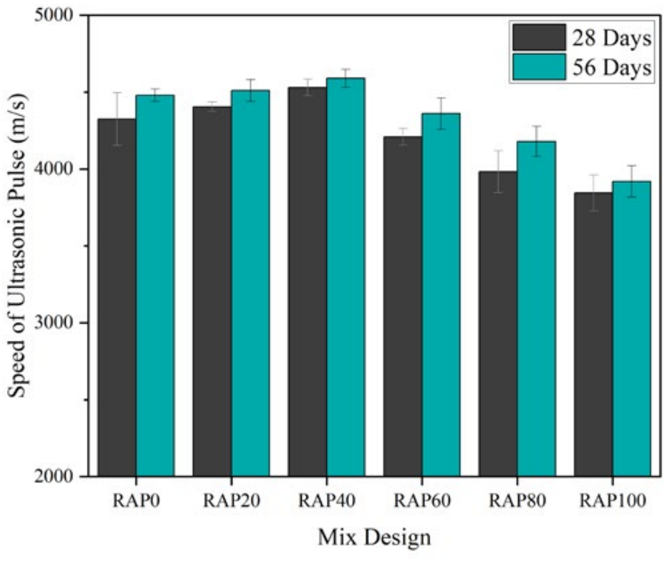

Figure 6. Ultrasonic pulse velocity of specimens at 28 days and 56 days (m/s).

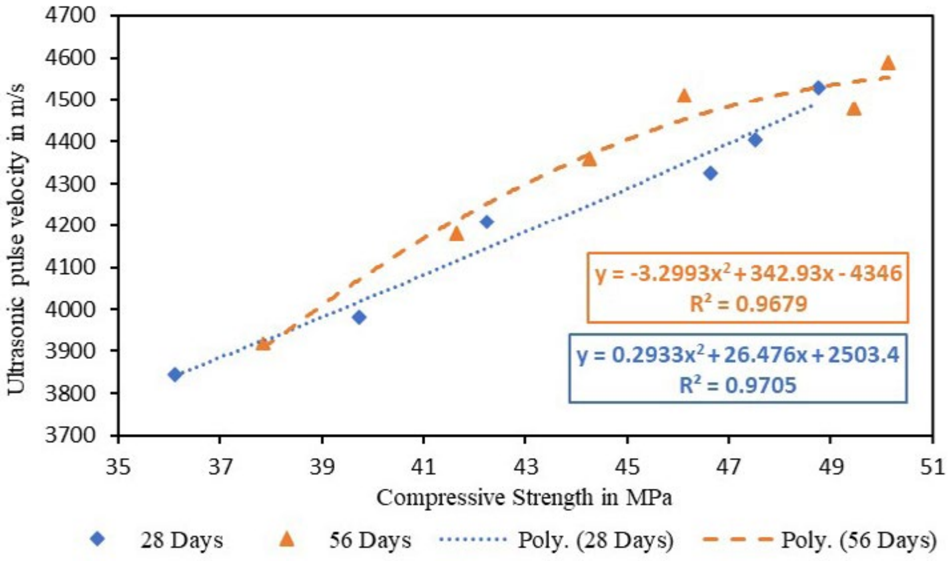

Figure 7. Correlation between Compressive strength ((N/mm^2) and Ultrasonic pulse velocity (m/s).

3.4. Initial surface absorption test

The initial surface absorption test is one of the most critical analyses to get insight into the performance and durability of GPC. The rate of unidirectional water infiltration through the surface of the GPC specimens.

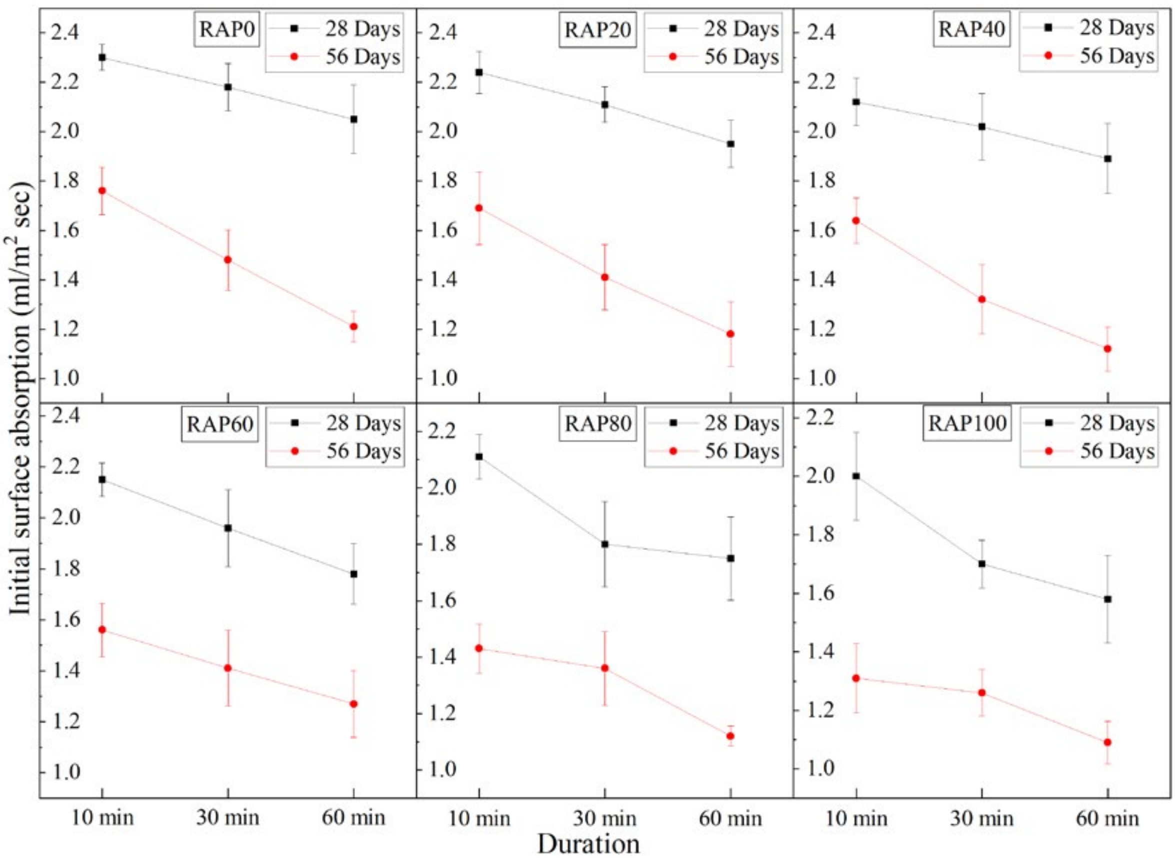

Figure 8. Initial surface absorption of geopolymer concrete (ml/m² sec).

It is used to calculate the absorption rate. Due to the frequent exposure of concrete surfaces to extreme environmental conditions, this examination is essential. Surface absorption resistance, therefore, becomes an important parameter for determining concrete durability. The absorption rates of the six different GPC mixes with varying percentages of RAP aggregate at curing ages of 28 and 56 days (10 mins, 30 mins, 60 mins) are graphically represented in Figure 8, along with their standard deviations. The GPC mix design RAP100 shows the surface absorption ranging from 1.09 ml/m²sec to 2.00 ml/m²sec at 28 days and 56 days collectively.

On the other hand, controlled mix RAP0 displays absorption ranging from 1.21 ml/m²sec to 2.3 ml/m²sec at 28 days and 56 days. RAP40 mix shows an absorption rate ranging from 1.12 ml/m²sec to 2.12 ml/m²sec at 28 days and 56 days of curing. It is noticeable that the initial surface absorption rate fluctuates with the percentage of RAP in the mix. Generally, as the RAP content increases, the rates tend to drop. This can be due to the unique characteristics of RAP, which might affect the porosity and surface absorption of the concrete. The findings also suggest that longer cure times frequently result in improved concrete performance and less absorption.

3.5. Microstructural and mineralogical analyses

3.5.1. Scanning electron microscope and energy dispersive spectroscopy

The scanning electron microscopy (SEM) combined with energy-dispersive spectroscopy (EDS) was employed to examine the microstructural characteristics of the 56-day-old geopolymer concrete, as shown in Figure 9 (a, b). The microstructure of RAP40, which incorporates 40% recycled asphalt pavement aggregate, displays a more cohesive and refined matrix compared to RAP0. Notably, the binder matrix appears denser and more continuous, with fewer microcracks and voids observed, particularly at the interfacial transition zones, as shown in Figure 9 (b). This enhanced microstructural integrity suggests a more effective geopolymerisation process and improved particle-paste bonding, likely facilitated by the reactive mineral content contributed by the RAP aggregate, fly ash and dolomite. EDS analysis of this region confirms the presence of key elements such as Si, Al, Na, Ca, Fe, and Mg, indicating the co-existence of both sodium aluminosilicate hydrate (N-A-S-H) and calcium aluminosilicate hydrate (C-A-S-H) gels.

The calcium and magnesium content observed in concrete suggests the beneficial contribution of dolomite-rich phases to the formation of C-A-S-H gel, which can enhance matrix densification and long-term strength development. In contrast, RAP0, which lacks RAP content, presents a comparatively less compact matrix, as shown in Figure 9 (a).

Although unreacted or partially reacted fly ash particles are surrounded by a geopolymeric binder, the gel distribution appears more discontinuous with visible micro-voids and incomplete matrix connectivity. EDS analysis reveals a composition dominated by Si, Al, Na, and O, indicating a primarily N-A-S-H gel formation with limited C-A-S-H contribution. The relatively lower elemental diversity and gel complexity may contribute to a less robust microstructure in RAP0, potentially affecting its mechanical performance under long-term exposure. Overall, the improved gel formation, microstructural compactness, and elemental synergy in RAP40 reflect its enhanced performance, demonstrating the beneficial role of RAP aggregate inclusion in the geopolymer concrete matrix.

This interpretation is well-supported by FTIR spectra, where absorption bands near 950–1100 cm^{-1} correspond to asymmetric Si-O-T (T = Al or Si) vibrations typical of geopolymer networks, as shown in Figure 11.

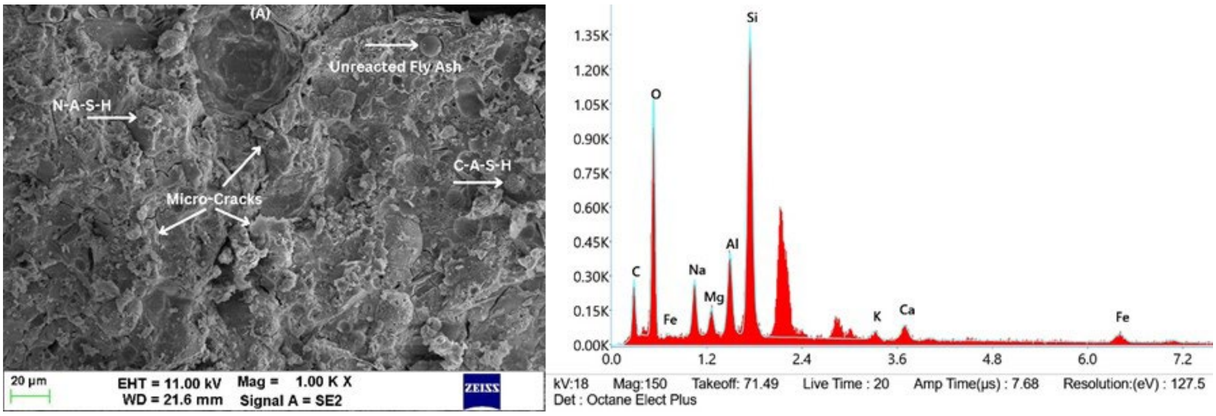

(a) SEM and EDS analysis of geopolymer concrete mix RAP0

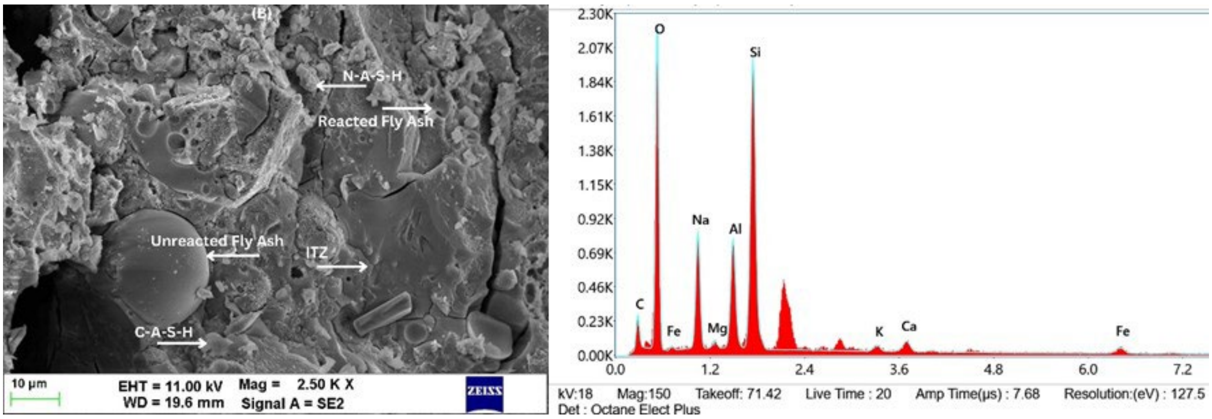

(b) SEM and EDS analysis of geopolymer concrete mix RAP40

Figure 9. SEM and EDS analysis of geopolymer concrete mix (a) RAP0 and (b) RAP40.

3.5.2. X-ray diffraction

X-ray diffraction (XRD) was employed to investigate the crystalline phases present in the geopolymer concrete systems, and the resulting diffractograms for RAP0 and RAP40 are shown in Figure 10. Both samples predominantly exhibit peaks corresponding to quartz (Q), with its most intense reflections observed at 2θ ≈ 26.84°, 36.74°, 50.32°, and 60.13°. These peaks are particularly sharper and more intense in RAP0, suggesting a higher fraction of unreacted crystalline silica, primarily originating from the raw fly ash and aggregates. In addition to quartz, minor peaks corresponding to mullite (M) at 2θ ≈ 16.63°, 21.11°, 26.14°, and calcite (C) at 2θ ≈ 29.68°, 39.65°, 48.86° detected, confirming the partial presence of thermally stable aluminosilicate and carbonate phases (34-36). The sharper and more numerous peaks in the RAP0 spectrum indicate a relatively crystalline matrix with limited geopolymeric reaction, consistent with the presence of residual mullite and calcite. This is further corroborated by microstructural SEM observations (Figure 9a), which revealed unreacted or partially reacted fly ash particles embedded within a porous and loosely bound matrix.

In contrast, the RAP40 sample displays a notable reduction in the intensity and sharpness of crystalline peaks, especially those of quartz and mullite. Furthermore, the appearance of a broad hump between 20° and 35° at 2θ, characteristic of an amorphous phase—indicates the formation of geopolymeric gel products aligning with SEM analysis as shown in Figure 9b. The diminished quartz peak intensities in RAP40 reflect enhanced dissolution of reactive silica and alumina facilitating more extensive geopolymerisation.

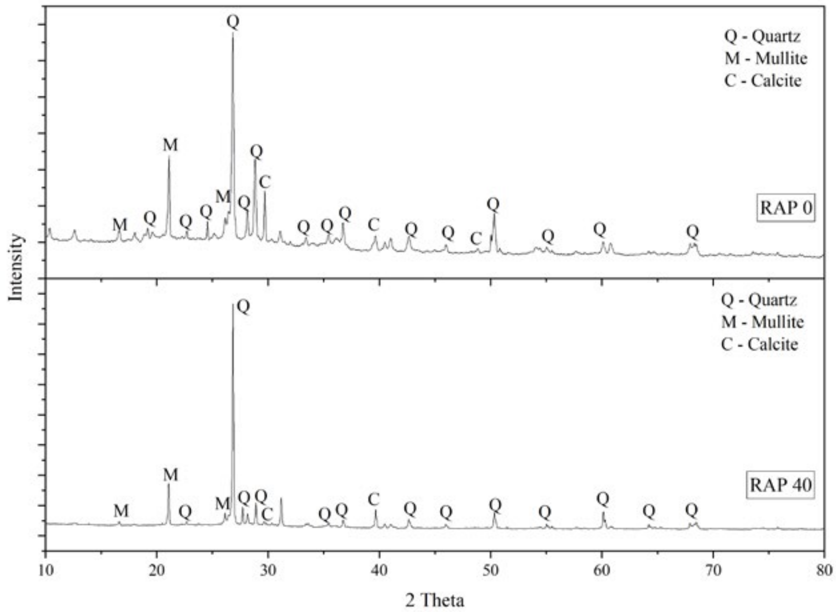

Figure 10. XRD analysis of geopolymer concrete mix RAP0 and RAP40.

3.5.3. Fourier transform infrared spectroscopy

Fourier Transform Infrared Spectroscopy (FTIR) was conducted to investigate the molecular bonding environment within the geopolymer matrix, as shown in Figure 11. Both RAP0 and RAP40 exhibit key absorption bands indicative of geopolymeric gel formation, with distinct differences in band intensity and position reflecting the degree of reaction and network development. In the RAP0 specimen, a broad and asymmetric absorption band is observed between 950-1100 cm^{-1}, attributed to the Si–O–T (T = Si or Al) asymmetric stretching vibrations, which are characteristic of the aluminosilicate network in sodium aluminosilicate hydrate (N-A-S-H) and calcium aluminosilicate hydrate (C-A-S-H) gels. However, the lower intensity and sharper features of these bands suggest a less polymerised and more heterogeneous gel phase. This interpretation is supported by SEM analysis, which shows unreacted or partially reacted fly ash particles and a relatively porous matrix, indicating incomplete geopolymerisation.

In contrast, RAP40 displays a noticeable shift and broadening of the main Si-O-T absorption band toward lower wavenumbers (around 950-1000 cm^{-1}), signifying a more extensive polymerisation and the evolution of a more developed aluminosilicate network. The enhanced gel formation is further evidenced by the compressive strength results as shown in Figure 2, which are also consistent with the XRD analysis, as shown in Figure 10, which shows suppressed crystalline quartz peaks and increased amorphous phase content. This suggests that more of the quartz and aluminosilicate phases have been consumed in the geopolymerisation process, resulting in a denser and more uniform binding matrix. Additional peaks in the range of 1400-1500 cm^{-1} correspond to C-O asymmetric stretching and H-O-H bending vibrations, respectively, associated with minor carbonate presence and adsorbed moisture. However, these bands are less pronounced and do not dominate the spectral features, indicating minimal interference in gel formation. Corroborated by SEM-EDS and XRD analyses, RAP40 exhibits a higher degree of geopolymer gel formation compared to RAP0. The broader Si-O-T bands observed in FTIR signify enhanced polycondensation, aligning with the denser microstructure identified via SEM and the lower crystalline intensity in XRD. These findings underscore that incorporating 40% RAP aggregate significantly improves the microstructural integrity and strength by promoting a more stable, amorphous aluminosilicate matrix.

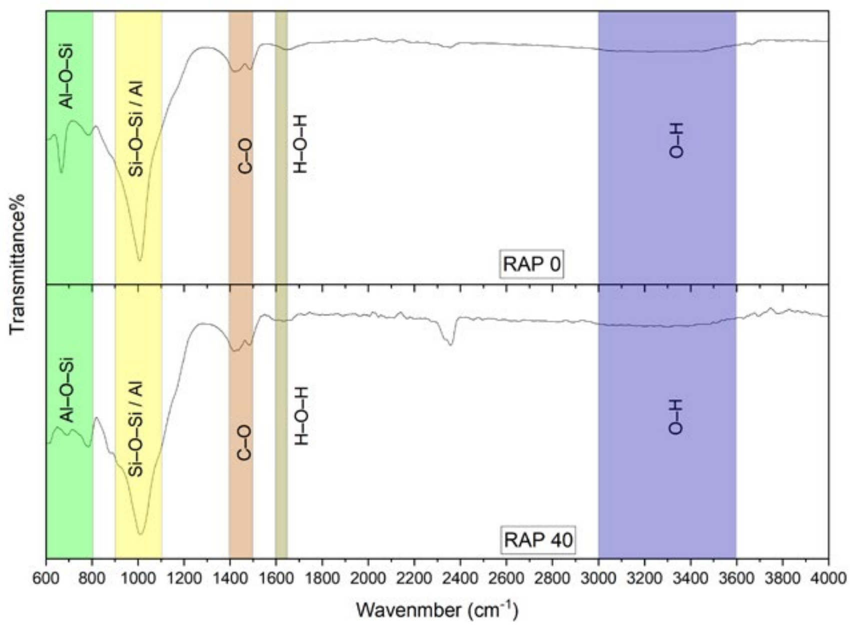

Figure 11. FTIR analysis of geopolymer concrete mix RAP0 and RAP40.

4. CONCLUSIONS

The study addresses complexities in RAP integration, emphasising the influence of waste source on its properties within the geopolymer matrix. Comprehensive strength assessments, along with morphological studies utilising advanced techniques such as SEM, EDS, XRD, and FTIR, provide a thorough understanding of RAP aggregate geopolymer concrete characteristics, contributing valuable insights into the intricate interplay of materials with varying ration of RAP aggregate and enhancing the scientific knowledge of waste management with sustainable construction practices.

The study establishes a strong correlation between compressive strength, flexural strength, split tensile strength, and initial surface absorption. The relationship is influenced by the percentage of recycled asphalt pavement aggregate ratio in geopolymer concrete.

The equations derived for the correlation between varying properties in correspondence to compressive strength at 28 and 56 days show high R^2 values near 1, signifying a significant and credible positive correlation.

RAP40 concrete mix displayed the highest compressive strength at 28 and 56 days, with an increase of 4.50% and 1.39%, respectively, over GPC with NA. Flexural strength exhibited a similar trend, with RAP40 leading at both ages, with an increase of 8.79% at 28 days and 1.04% at 56 days. Establishing a positive correlation using the power equation $R^2 = 0.9127$ and $R^2 = 0.9879$ for 28 and 56 days.

Similarly, in the split tensile strength test, RAP40 showed the highest values at both ages, increasing 6.54% at 28 days and 1.02% at 56 days. Using power equations, a positive correlation was established with compressive strength, with R^2 values of 0.9597 and 0.9118 for 28 and 56 days, respectively.

This study also reveals a noteworthy correlation between compressive strength and ultrasonic pulse velocity, with R^2 values of 0.9705 for 28 days and 0.9679 for 56 days. The increment in results observed for RAP40 was about 12.72% for 28 days and 9.25% for 56 days. This increment relates to the dense structure and the increased strength of GPC.

Longer curing periods lead to better concrete performance and reduced absorption, as observed in the initial surface absorption test. An average drop in the RAP40 mix is seen as 7.65% for 28 days and 8.34% for 56 days; for RAP100, an average declining value of 10.49% and 13.61% for 28 and 56 days is recorded. This is due to the presence of an asphalt coating over aggregate.

The mineralogical and microstructural investigation demonstrates superior performance of RAP40 over RAP0 in geopolymer concrete, as revealed by SEM-EDS, XRD, and FTIR analyses. RAP40 exhibits enhanced mineralogical complexity with the formation of critical hydrates (C-A-S-H and N-A-S-H).

XRD data confirm that the inclusion of 40% RAP promotes a higher degree of geopolymerisation, evidenced by increased amorphous content and reduced crystalline residue. FTIR unveils transformative geopolymerisation in RAP40 with Si–O–T (T = Si or Al) peaks, aligning with EDS and solidifying RAP40's superiority in performance and composition.

Supplementary information ↑

Funding sources

The author declares that no funding was received from any agency, institution, or organisation for conducting this research.

Supplementary material

Not applicable.

Data availability

Not applicable.

Acknowledgements

Not applicable.

Authorship contribution statement

Sajan Sharma: Conceptualisation, data cleansing, methodology, visualisation, formal analysis, research, write-up – original draft.

Shailja Bawa: Supervision, conceptualisation, write up-review & editing, validation, resources.

Competing interests

The authors of this article declare that they have no financial, professional or personal conflicts of interest that could have inappropriately influenced this work.

Statement on the use of Artificial Intelligence

Not applicable.

REFERENCES

1. NAPA. 2023. National Asphalt Pavement Association LMU.
2. Chandra S. Flexible Pavement versus Rigid Pavement. CSIR Central Road Research Institute, Delhi.
3. Ali H, Rojali A. 2023. Recycling asphalt pavements: the state of practice. In: Recycling strategy and challenges associated with waste management towards sustaining the world. https://doi.org/10.5772/intechopen.106235
4. McDaniel RS, Shah A, Huber GA, Copeland A. 2012. Effects of reclaimed asphalt pavement content and virgin binder grade on properties of plant produced mixtures. *Road Mater Pavement Des*. 13(sup1):161–182. https://doi.org/10.1080/14680629.2012.657066
5. Silva HMRD, Oliveira JRM, Jesus CMG. 2012. Are totally recycled hot mix asphalts a sustainable alternative for road paving? *Resour Conserv Recycl*. 60:38–48. https://doi.org/10.1016/j.resconrec.2011.11.013

6. Federal Highway Administration Research and Technology. User Guidelines for Waste and Byproduct Materials in Pavement Construction. Washington, DC, USA.

7. Puppala AJ, Saride S, Williammee R. 2012. Sustainable reuse of limestone quarry fines and RAP in pavement base/subbase layers. *J Mater Civ Eng*. 24(4):418–429. https://doi.org/10.1061/(ASCE)MT.1943-5533.0000404

8. Singh S, Ransinchung GD, Kumar P. 2017. Effect of mineral admixtures on fresh, mechanical and durability properties of RAP inclusive concrete. *Constr Build Mater.* 156:19–27. https://doi.org/10.1016/j.conbuildmat.2017.08.144

9. Abedalqader A, Shatarat N, Ashteyat A, Katkhuda H. 2021. Influence of temperature on mechanical properties of recycled asphalt pavement aggregate and recycled coarse aggregate concrete. *Constr Build Mater.* 269:121285. https://doi.org/10.1016/j.conbuildmat.2020.121285

10. Erdem S, Blankson MA. 2014. Environmental performance and mechanical analysis of concrete containing recycled asphalt pavement and waste precast concrete as aggregate. *J Hazard Mater.* 264:403–410. https://doi.org/10.1016/j.jhazmat.2013.11.040

11. Abdel-Mohti A, Shen H, Khodair Y. 2016. Characteristics of self-consolidating concrete with RAP and SCM. *Constr Build Mater.* 102:564–573. https://doi.org/10.1016/j.conbuildmat.2015.11.007

12. Soltanabadi R, Behfarnia K. 2022. Shear strength of reinforced concrete deep beams containing recycled concrete aggregate and recycled asphalt pavement. *Constr Build Mater.* 314:125597. https://doi.org/10.1016/j.conbuildmat.2021.125597

13. Liu H, Duan G, Wang F, Zhang J, Zhou Y, Feng Y, Zhang K. 2022. Investigation on mechanical behaviors of Self-compacting concrete containing reclaimed asphalt pavement. *Constr Build Mater.* 346:128421. https://doi.org/10.1016/j.conbuildmat.2022.128421

14. Scrivener KL, John VM, Gartner EM. 2018. Eco-efficient cements: potential economically viable solutions for a low-CO_2 cement-based materials industry. *Cem Concr Res*. 114:2–26. https://doi.org/10.1016/j.cemconres.2018.03.015

15. Dixit S, Arora R, Kumar K, Bansal S, Vatin N, Araszkiewicz K, Epifantsev K. 2022. Replacing e-waste with coarse aggregate in architectural engineering and construction industry. *Mater Today Proc*. 56(4): 2353-2358. https://doi.org/10.1016/j.matpr.2021.12.154

16. Podolsky Z, Liu J, Dinh H, Doh JH, Guerrieri M, Fragomeni S. 2021. State of the art on the application of waste materials in geopolymer concrete. *Case Stud Constr Mater.* 15:e00637. https://doi.org/10.1016/j.cscm.2021.e00637

17. Avirneni D, Peddinti PRT, Saride S. 2016. Durability and long-term performance of geopolymer stabilized reclaimed asphalt pavement base courses. *Constr Build Mater.* 121:198–209. https://doi.org/10.1016/j.conbuildmat.2016.05.162

18. Hoy M, Horpibulsuk S, Arulrajah A. 2016. Strength development of recycled asphalt pavement–fly ash geopolymer as a road construction material. *Constr Build Mater.* 117:209–219. https://doi.org/10.1016/j.conbuildmat.2016.04.136

19. Hoy M, Rachan R, Horpibulsuk S, Arulrajah A, Mirzababaei M. 2017. Effect of wetting–drying cycles on compressive strength and microstructure of recycled asphalt pavement–fly ash geopolymer. *Constr Build Mater.* 144:624–634. https://doi.org/10.1016/j.conbuildmat.2017.03.243

20. Rahman SS, Khattak MJ. 2020. Mechanical and durability characteristics of roller compacted geopolymer concrete using reclaimed asphalt pavement. *Proceedings of the International Conference on Civil Infrastructure and Construction (CIC)*, *2020*(1), 420–430. https://doi.org/10.29117/cic.2020.0053

21. Rahman SS, Khattak MJ. 2022. Feasibility of reclaimed asphalt pavement geopolymer concrete as a pavement construction material. *Int J Pavement Res Technol*. 16:888-907. https://doi.org/10.1007/s42947-022-00169-8

22. ASTM C127-88. Standard Test Method for Specific Gravity and Absorption of Coarse Aggregate.

23. ASTM C128-01. Standard Test Method for Density, Relative Density (Specific Gravity), and Absorption of Fine Aggregate.

24. ASTM C136-06. Standard Test Method for Sieve Analysis of Fine and Coarse Aggregates.

25. ASTM C430-08. Standard Test Method for Fineness of Hydraulic Cement by the 45-µm (No. 325) Sieve.

26. ASTM C618-12a. Standard Specification for Coal Fly Ash and Raw or Calcined Natural Pozzolan for Use in Concrete. https://doi.org/10.1520/C0618-12a

27. ASTM C25-11. Standard Test Methods for Chemical Analysis of Limestone, Quicklime, and Hydrated Lime. https://doi.org/10.1520/C0025

28. IS 516 (Part 1/Sec 1). 2021. Hardened Concrete Methods of Test.

29. BIS:5816. 1999. Specification for splitting tensile strength of concrete -Method of Test, New Delhi, India.

30. BS 1881: Part 208. 1996. Testing concrete Part 208. Recommendations for the determination of the initial surface absorption of concrete.

31. ASTM C597-02. Standard Test Method for Pulse Velocity Through Concrete. https://doi.org/10.1520/C0597-09

32. Kılıç D, Öz A, Benli A, Tortum A, Kaplan G, Aydın AC. 2025. Integration of reclaimed asphalt aggregates into glass fiber-reinforced alkali-activated composites: mechanical performance and durability. *Constr Build Mater*. 458:139645. https://doi.org/10.1016/j.conbuildmat.2024.139645

33. Ghosh A, Ransinchung G, Kumar P, Zaw CHH. 2024. Effect of particle size and proportion of RAP aggregates on strength, durability and microstructure of ambient cured geopolymer concrete mixes. *Constr Build Mater*. 455:139164. https://doi.org/10.1016/j.conbuildmat.2024.139164

34. Donatello S, Kuenzel C, Palomo A, Fernández-Jiménez A. 2014. High temperature resistance of a very high volume fly ash cement paste. *Cem Concr Compos*. 45:234–242. https://doi.org/10.1016/j.cemconcomp.2013.09.010

35. Lin M, Chen G, Chen Y, Han D, Su R, Wu J. 2025. Mechanical properties and microstructure of fly ash and slag-based geopolymer prepared by silica fume-based activator. *J Clean Prod*. 498:145214. https://doi.org/10.1016/j.jclepro.2025.145214

36. Wojtacha-Rychter K, Cempa M, Król M, Kiełbasa K, Zhang L, Liu R, Smolinski A. 2025. Modified fly ash-based geopolymer as a sustainable solution for ammonia storage by sorption. *Ind Crops Prod*. 230:121057. https://doi.org/10.1016/j.indcrop.2025.121057